EFFECTS OF THE VARIATION OF THE EXCITATION AND BOUNDARY CONDITIONS OF MODE-STIRRED CHAMBERS AND CONSEQUENCES FOR CALIBRATION AND MEASUREMENTS

H.G.Krauthäuser, J.Nitsch
Otto-von-Guericke-University Magdeburg, IGET, Germany
(Principal contact: hgk@ieee.org)

Abstract: Field transients are an intrinsic feature of mode-stirred chambers. Three different cases are investigated here. The free energy decay corresponds to transients on a microsecond time scale. The time for transients due to a change of frequency depends on the equipment used. In any case it is significantly longer, usually several milliseconds. If a mechanical tuner is used to change the boundary conditions, due to the inertia of the construction, transients occur within a time period up to several seconds whenever the tuner is moved to a new position. All these field transients may affect equipment under test. Moreover, the free energy decay can be used to determine the chamber quality factor in the time domain. For this task, a method, using a spectrum analyzer instead of an oscilloscope, is introduced leading to a much higher dynamic range.

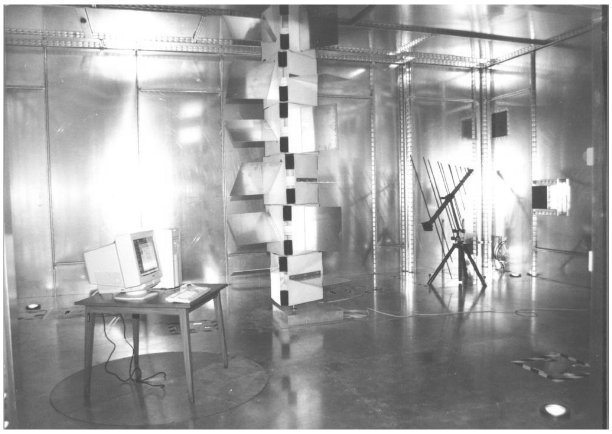

Fig. 1: Picture of the Magdeburg mode-stirred chamber.

1. Introduction

During the last few years, mode-stirred chambers have become more and more popular for radiated emc testing. For susceptibility testing this is mainly due to the fact that very high field strengths can be achieved with moderate input power. Both, for susceptibility and emission testing, the statistic nature of the chamber fields might be helpful to perform more robust tests, especially at high frequencies (above 1 GHz).

An international standard — IEC 61000-4-21 — is in development dealing both with the calibration of mode-stirred chambers and mode-stirred chamber measurements.

The main future research task is to investigate real and generic systems in mode-stirred chambers and to compare the results with measurements performed in well established test environments, namely open area test sides (OATS), semi or fully anechoic chambers (SAC, AC), or transversal electromagnetic wave guides (TEM-cell, GTEM-cell, strip line).

Mode-stirred chambers are high quality resonators. According to the high quality factors, steady state conditions are reached only after a considerable long time period, typically several microseconds (Figure 5 shows the quality factor and the chamber time constant for the Magdeburg mode-stirred chamber). Although this is the shortest time period of transients existing in mode-stirred chambers, it might be already a long time for fast digital electronics [1]. Therefore, field transients in mode-stirred chambers might be important for the interpretation of emc test results.

The measurements presented here are conducted in the Magdeburg mode-stirred chamber [2]. The chamber dimensions are 8 m x 6 m x 3.5 m, approximately. The first chamber resonance frequency is about 30 MHz. The chamber is calibrated according to IEC 61000-4-21 in the frequency range from 200 MHz to 4.2 GHz.

In the next section, the free energy decay is investigated. From the slope of the free decay the chamber quality factor and the chamber time constant are evaluated for the empty and the heavily loaded chamber.

Most emc tests in reverberation chambers are performed in mode-tuned operation. In that mode, the tuner is sequentially moved to statistically independent positions. At these positions, the test is performed for all frequencies without moving the tuner. For these frequency sweeps, the generator can be set to blanking or non-blanking operation. In the second part, field transients due to the change of the frequency are investigated, both for blanking and non-blanking operation.

The oscillations of the (mechanical) tuner are relevant on a much longer time scale (seconds). Field transients due to tuner oscillations are described in the third part of the

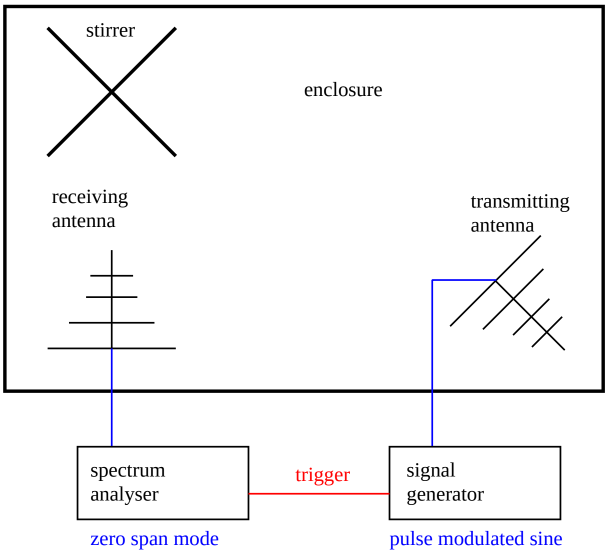

Fig. 2: Setup for Q-factor measurements in time domain.

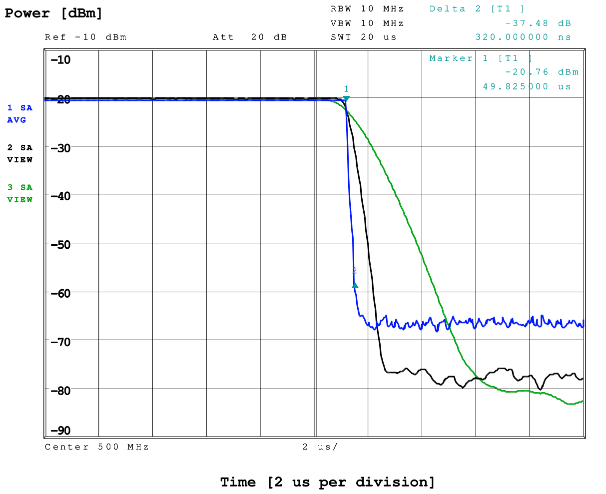

Fig. 3: Slope of the pulse-modulated sine signal when the generator is directly connected to the spectrum analyzer. The three traces are for resolution bandwidths of 10 MHz, 1 MHz, and 300 kHz.

paper.

All measurements presented here are performed without the use of amplifiers. Generally, amplifiers will cause additional effects due their own transient behavior.

2. Free Energy Decay

2.1 Quality factor from time domain measurements

The quality factor Q is one of the most known parameters to characterize reverberation chambers. In general, Q is defined by

$$Q = \omega \frac{\text{overall reactive energy in the enclosure}}{\text{dissipated power}} \quad . \tag{1}$$

In time domain, the quality factor is given by

$$Q = \frac{\pi}{d} = 2\pi f \cdot \tau \tag{2}$$

where d is the average logarithmic decrement of the free-decay field of energy density stored in any point of the enclosure [3]:

$$\begin{aligned} d &= \frac{1}{f \cdot \Delta t} \ln\left(\frac{E(t_0)}{E(t_0 + \Delta t)}\right) && (3)\\ &= \frac{\ln(10)}{20 \cdot f \cdot \Delta t} \Delta E_{dB} && (4)\\ &= \frac{\ln(10)}{20 \cdot f \cdot \Delta t} \Delta P_{dB} && (5) \end{aligned}$$

The energy (field) decay time constant τ is given by

$$\begin{aligned} \langle E(t_0 + \tau) \rangle &= (1/\sqrt{e}) \, \langle E(t_0) \rangle && (6)\\ \langle E_{dB_{V/m}}(t_0 + \tau) \rangle &= \langle E_{dB_{V/m}}(t_0) \rangle - 4.34 dB_{V/m} && (7) \end{aligned}$$

From (5) and (2) follows

$$Q = \frac{20 \cdot \pi \cdot f[\text{MHz}] \cdot \Delta t[\mu s]}{\ln 10 \cdot \Delta P_{dB}} \approx 27.29 \cdot \frac{f[\text{MHz}] \cdot \Delta t[\mu s]}{\Delta P_{dB}} \tag{8}$$

To perform the time domain measurements it would be obvious to use a real-time or a sampling oscilloscope. This technique was introduced by Ladbury, Johnk and Ondrejka at NIST in 1996 [4]. The disadvantages of the method is a relative complex data processing and that it can be hardly used at high frequencies due to the lack of a pulse source with strong signal components at several GHz and the poor dynamic range of high speed oscilloscopes (8 bit analog digital conversion).

Here, a new method is introduced using a modern spectrum analyzer in zero span mode (in zero span mode the analyser measures the signal at the given center frequency with the given band width as a function of time) and an excitation with a pulse modulated sine. The setup is illustrated in Fig. 2.

Performing the measurements it is important to use a resolution bandwidth for the spectrum analyzer that is large enough to get the correct slope of the envelope. For the measurements here the maximum resolution bandwidth (10 MHz) of the used spectrum analyzer (Rhode&Schwarz FSP13) was taken. In order to check whether the bandwidth is large enough or not, the slope of the envelope can be measured when the generator is directly connected to the spectrum analyzer. The resulting slope has to be much steeper compared to the chamber measurements. The resulting slopes for different values of the resolution bandwidth are illustrated in Fig. 3. From Eq. 8 using the values $\Delta t = 320$ ns and $\Delta P_{dB} = 37.48$ dB it can be calculated how large the quality factor has to be at least to be measured with this method correctly. This lower Q limit, Q_{min}, is given in Fig. 4 for frequencies up to 20 GHz.

Measured slopes are given in Fig. 5 (top) for five different positions of the tuner (the curves have been shifted on the time axis in order to clarify the illustration). For the results given here the chamber was heavily loaded with absorbing material. The free-decay slopes are of complex structure making the determination of the decay time practically impossible and/or inaccurate.

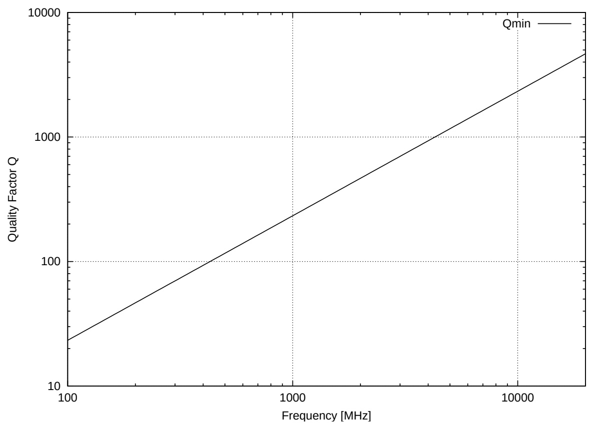

Fig. 4: Minimum value of the quality factor Q that can be measured by means of a spectrum analyzer in zero span mode using a resolution bandwidth of 10 MHz.

The idea is now to average the slopes for different tuner positions in order to get an ensemble slope that should be much smoother than the individual curves. This can be achieved most easily in mode-stirred operation of the chamber.

In contrast to mode-tuned operation in mode-stirred operation the tuner is moved continously. Therefore, the ensemble averaged slope is obtained by using the internal averaging capability of the spectrum analyzer. The resulting ensemble average curve is given in Fig. 5 (top) also.

The bottom graph of Fig. 5 shows the resulting quality factors and decay time constants for the empty and heavily loaded chamber, respectively. The obtained Q is clearly above the limit from Fig. 4.

In order to validate the new method, the results can be compared to theoretical models for the quality factor and to the results obtained using the well established method (as in IEC 61000-4-21).

2.2 Quality factor from simple theory

Following an easy but well established theoretical model the quality factor is given by two parts [5], [6]:

$$Q_{th} = \frac{1}{\frac{1}{Q_{ant}} + \frac{1}{Q_{wall}}} \tag{9}$$

$$Q_{ant} = 16\pi^2 \frac{V}{\lambda^3} \tag{10}$$

$$Q_{wall} = \frac{3}{2}\frac{V}{S\delta}\frac{1}{1+\frac{3\lambda}{16}\left(\frac{1}{a}+\frac{1}{b}+\frac{1}{c}\right)} \tag{11}$$

where V and S are the volume and surface of the chamber, a, b, c are the dimensions of the chamber (that is assumed to be cubic), $\lambda = c/f$ is the wavelength, c is the speed of light, f is the frequency and $\delta = \sqrt{\frac{\lambda}{c\mu\sigma}}$ is the skin depth of the wall with permeability μ and conductivity σ.

The two parts are due to effects of the receiving antenna (Q_{ant}) and wall losses (Q_{wall}).

For real chambers an additional factor K has to be introduced giving the ratio between measured and modeled Q factors:

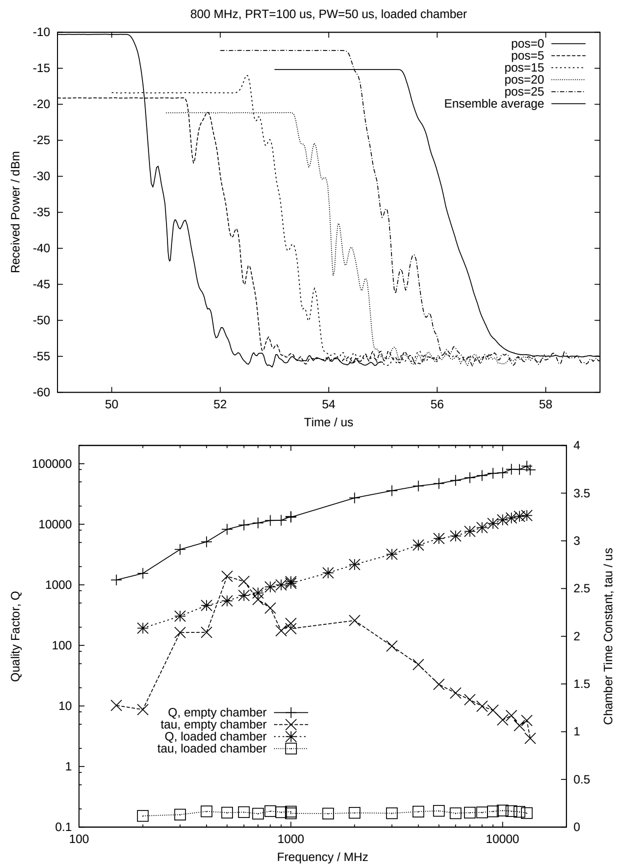

Fig. 5: Top: Time domain response due to pulse modulated sine excitation of the (loaded) chamber. Bottom: Chamber quality factor Q and decay time constant τ for the Magdeburg mode-stirred chamber.

$$K = \frac{Q_{th}}{Q_{meas}} \tag{12}$$

In order to compare the measured Q with respect to the theoretical model, values for σ, μ and K have to be chosen. The Magdeburg mode-stirred chamber is made from screwed zinc coated steel modules. Due to the modular structure, a value for the (effective) conductivity can not be obtained from the conductivity of the material itself. In Fig. 6 the measured quality factor is compared to the prediction of the model using $\sigma = 1e6S/m$, $\mu = \mu_0$ and $K = 3.5$. With these parameters a good agreement is obtained.

2.3 Quality factor from frequency domain measurements

Usually, the quality factor of mode-stirred chambers is measured in the frequency domain using the formula

$$Q = \left(\frac{16\pi^2 V}{\eta_{Rx}\eta_{Tx}\lambda^3}\right)\left\langle\frac{P_{AvgRec}}{P_{inp}}\right\rangle_{\text{antenna locations}} \tag{13}$$

Here, η_{Rx} and η_{Tx} are antenna efficiency factors for the receiving (Rx) and transmitting (Tx) antenna. These factors can be set approximately to 0.75 for log-periodical and 0.9 for aperture (horn) antennas. P_{AvgRec} is the power at the receiving antenna averaged over

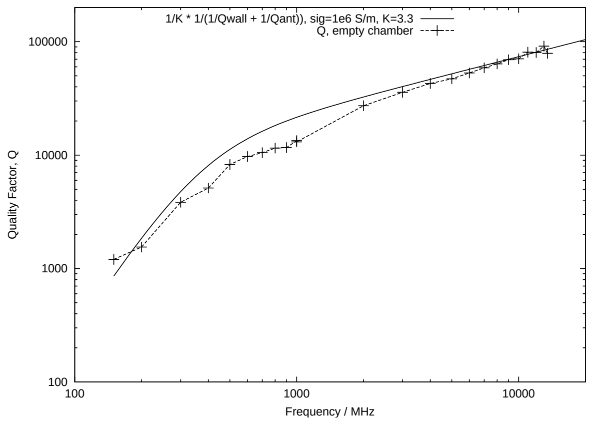

Fig. 6: Comparison of the measured quality factor with the prediction of a simple theoretical model using losses due to the receiving antenna and wall losses.

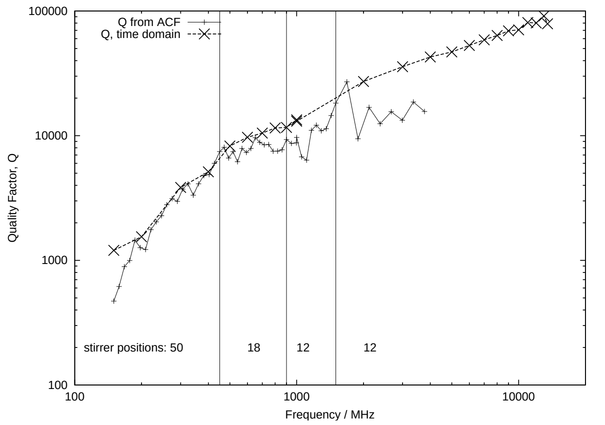

Fig. 7: Comparison of the empty chamber quality factor over frequency obtained in the frequency domain from the antenna calibration factor (ACF) as described in IEC 61000-4-21 and from time domain measurements using a spectrum analyzer in zero span mode with pulse modulated sine excitation (mode stirred operation).

tuner positions, P_{inp} is the chamber input power, and $\langle\rangle_{\text{antenna locations}}$ denotes averaging over different positions of the receiving antenna in the chamber working volume. The Q factor is obtained during chamber calibration according to IEC-61000-4-21 from the antenna calibration factor $ACF = \left\langle \frac{P_{AvgRec}}{P_{inp}} \right\rangle_{\text{antenna locations}}$.
In Fig. 7 the quality factor obtained from the ACF is compared to the quality factor measured in the time domain.

For frequencies up to 450 MHz both measurements are in excellent agreement. Above 450 MHz the number of tuner positions was reduced to 18 up to 900 MHz and to 12 above 900 MHz (as suggested in IEC 61000-4-21). The discrepancy between the two measurements in this frequency range may be due to an systematic underestimation of P_{AvgRec}. Above 4.2 GHz no frequency domain data is available due to the lack of power amplifiers for higher frequencies.

Above it was discussed how field transients, due the free energy decay inside mode-stirred chambers, can be used to determine the chamber quality factor Q. Beside this, the transients may also cause an unwanted influence on equipment under test. Transients as observed for the free energy decay occur whenever the electromagnetic conditions of the chamber are changed. Depending on whether the foregoing steady state is near to resonance conditions or not, much higher field amplitudes can be obtained during the transition to the next steady state. An example is given in the magnified part of the bottom graph of Fig. 8. There, the maximum amplitude is about 6.5 dB higher as in the steady state. These peaks are present only for a time up to approximately 100 ns. Therefore, this effect may upset only very fast (digital) equipment.

It is shown in the next sections, that much longer transition times can be observed in the case of changing the excitation frequency or the boundary conditions (tuner movement).

3. Change of Frequency

All emc susceptibility testing has to be done over a wide frequency range. In a mode-stirred chamber, mode-tuned operation is usually used, were for fixed boundary conditions the frequency of the excitation is subsequently set to the desired frequencies. The focus of this section is the time period while the frequency changes from one setting to another.

Modern high frequency generators are capable to perform frequency sweeps. Depending on the model several operation modes can be distinguished:

- Non blanking operation only: Here, the output power is not reduced during the time within the generator changes the frequency.
- Blanking operation: The generator reduces the output power (e.g. 80 dB attenuation) while it changes the frequency. Usually, this results in a much slower sweep.
- Automatic switching between blanking and non-blanking operation depending on the step width.
- Configurable frequency sweep: User can define, whether to use blanking or non-blanking operation.

Of course, the same blanking and non-blanking operation modes can be realized manually[1].

Generally, blanking sweeps are slower than non-blanking sweeps. But for typical tests, the overall sweep time is defined by the dwell time, that is much longer than the transition time. Nevertheless, most remote control software for emc susceptibility testing does not use blanking sweeps. If the tests are performed inside the usual (non reverberating) emc field generators, the difference is unimportant in most cases. But this is completely different in mode-stirred chambers.

The differences for the fields inside a reverberating enclosure are illustrated in Fig. 8.

In the upper graph the power at the receiving antenna is shown for fixed antenna and tuner positions while the frequency is changed from 205 MHz to 210 MHz. A transient region is observed for a time period of approximately 1 ms. Depending on the frequency range, the frequency step, and the tuner position, the transients can look completely different. For the example given in Fig. 8, the field strength during the transient time period is

[1] The term manual is used only to distinguish from predefined sweeps. Of course, the manual setting of the frequency is done remotely by a measuring software most often.

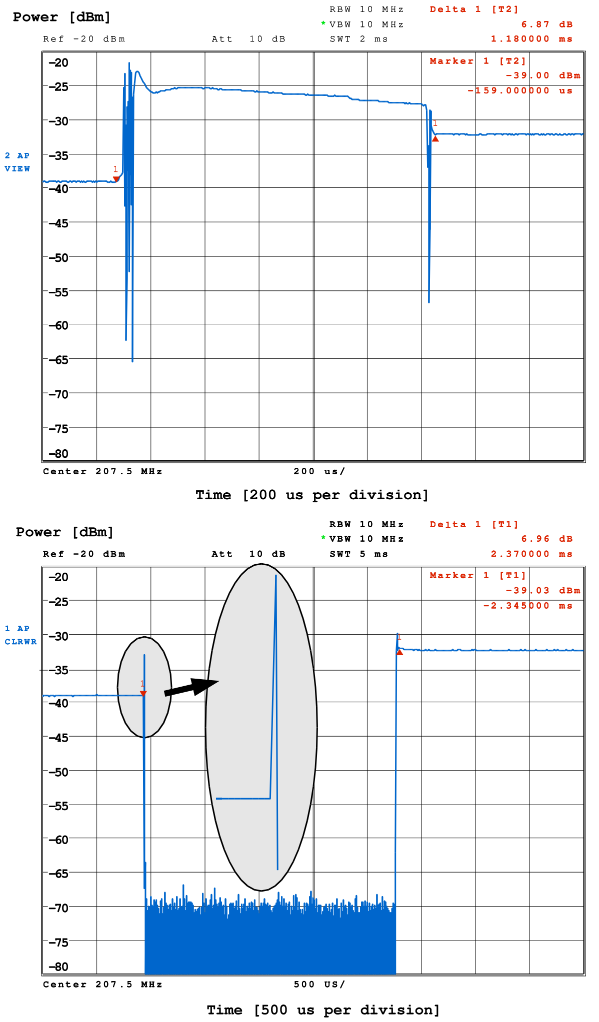

Fig. 8: Transient E-field during a frequency step from 205 MHz to 210 MHz. Top: without blanking; Bottom: with blanking. The enlarged part shows the transient due to the free energy decay when the power is reduced.

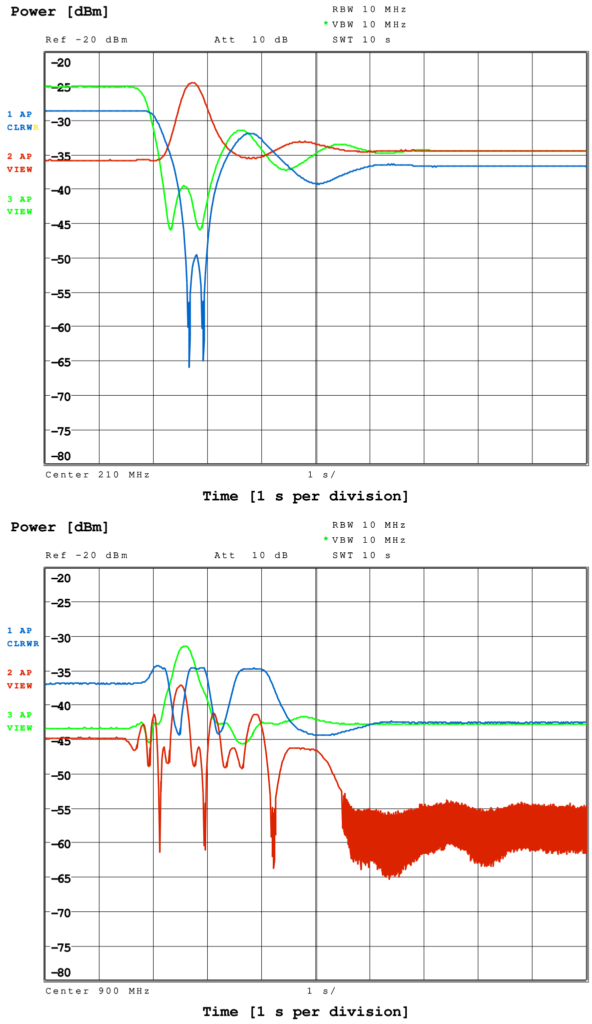

Fig. 9: Transient E-field due to the tuner movement to a new position. Step width is 5 degrees here. Top: at 200 MHz; Bottom: at 900 MHz

up to 10 dB higher compared to the corresponding steady state fields.

Obviously, this could cause an unwanted and uncontrolled upset of the equipment under test if a failure mechanism exists having a time constant less or equal to the transient time. In that case, a failure would be misleadingly addressed to the previous steady state.

These systematic over testing errors can be eliminated using banking frequency sweeps. The lower graph of Fig. 8 shows the same situation with blanking. The transient time is now 2.4 ms (using a Rhode&Schwarz SMR20). Amplitudes higher than steady state amplitudes are observed only for very short times (approximately 100 ns, see magnified part) at the moments when the power is reduced and reset (free energy decay). These shorter transients are important only for very hight speed digital circuits.

4. Tuner Movement

Most mode-stirred chambers are equipped with one or more mechanical tuners. These tuners ought to be large in order to perform well, even at lowest usable chamber frequencies. Due to the size and weight, tuners usually are inertial and tend to oscillate on a time scale of seconds.

This can be observed for the Magdeburg mode-stirred chamber also. This chamber is equipped with one large vertical tuner (see Fig. 1).

In order to demonstrate the effect, the tuner was moved from one position to another using a step width of 5 degrees. This has been done at different excitation frequencies. The field inside the chamber has been observed by means of a receiving antenna at a fixed position inside the chamber working volume.

Typical results are shown in Fig.9. The upper graph shows the received power for an excitation frequency of 200 MHz for three different starting positions of the tuner. Of course, the field amplitude inside the transient region strongly depends on the actual starting position. After approximately 1.5 seconds damped sine oscillations can be observed indicating that the tuner has taken the new position and is oscillating until steady state is reached. The overall transient time is about four seconds. For the lower graph the same measurements are made at a frequency of 900 MHz. The overall behavior is the same, but due to the much higher mode density the amplitude

pattern in the transient region is much more complex.
In any case, transient amplitudes can be observed that are up to 10 dB higher compared to the corresponding steady state amplitudes.
As discussed for frequency changing without blanking, the transient fields result in a systematic over testing with errors up to 10 dB. Here, this effect is important for equipment under test having failure mechanisms with time constants up to several seconds. This will include most of the typical equipment under test.

5. Conclusions

The phenomena of field transients are an immanent feature of high quality resonators, such as mode-stirred chambers. There are transient fields whenever either excitation parameters (e.g. frequency and amplitude) or the boundaries are changed.
Changing of the amplitude takes place when, e.g., the chamber is operated with a (pulse) modulated signal. The corresponding transients of the free energy decay can be used to determine the chamber quality factor in the time domain, and, on the other hand, might upset the device under test.
To determine the free energy decay a method was introduced using a spectrum analyzer in zero span mode instead of an oscilloscope. The results of the new method were compared to the established frequency domain method, and a simple theoretical method, showing that it is accurate, fast, simple, and can be used without amplifiers over a very broad frequency region. Values for the lowest quality factor to be measured with this method (assuming a resolution band width of 10 MHz) are given.
It was discussed that the field transients due to the free energy decay are important only for very fast digital circuits.
The change of the frequency is necessary in emc testing. The time period until steady state conditions are reached again depends on the used equipment (generator, amplifiers), and is in any case significantly larger (milliseconds) than the free energy decay time constant (microseconds). Obviously, these transients can disturb the device under test also. Care must be taken, to switch down power during this time period, e.g., by the measurement software. If frequency sweeps are done in non-blanking mode, systematic, unwanted and uncontrolled over testing (up to 10 dB) takes place. This will make a comparison of test results in mode stirred chambers and non-reverberating field generators even more complicated.
On a much larger time scale are the oscillations of a mechanical tuner (seconds). If mechanical tuners are used, power has to be switched down until the tuner is standing still. The time scale of this process will be important for most devices under test.
It is proposed to include proper measurement instructions into IEC 61000-4-21 as soon as possible.
This research is supported by the Deutsche Forschungsgemeinschaft DFG under contract number FOR417.

References

[1] Ch. Braun, P. Guidi, H.U. Schmidt, A. Taenzer, H. G. Krauthäuser, and J. Nitsch, "Messung von Ausfall-Schwellwerten an modernen Hochgeschwindigkeits-Prozessor-platinen mit gepulsten Hochleistungs-Mikrowellen und in Moden-Verwirbelungs-Kammern," in *Elektromagnetische Verträglichkeit EMV 2000*, Düsseldorf, Germany, 2000, pp. 573–580.

[2] H. G. Krauthäuser and J. Nitsch, "Characterization of mode-stirred chambers in the time domain," in *Proceedings of the International Symposium on EMC*, Magdeburg, Germany, Oct. 1999, pp. 389–392.

[3] P. Corona, L. Gaetano, and E. Paolini, "Performance and analysis of a reverberating enclosure with variable geometry," *IEEE Transactions on EMC*, vol. EMC-22, no. 1, pp. 2–5, 1980.

[4] R.T. Ladbury, J.M. ans Johnk and A.R. Ondrejka, "Rapid evaluation of mode-stirred chambers using impulsive waveforms," NIST Technical Note 1381, NIST, 1996.

[5] M.L. Crawford and G.H. Koepke, "Design, evaluation, and use of a reverberation chamber for performing electromagnetic susceptibility/vulnerability measurements," Tech. Rep. 1092, National Bureau of Standards, 1986.

[6] M.O. Hatfield, G.J. Freyer, and M.B. Slocum, "Reverberation characteristics of large welded steel shielded enclosures," in *Proceedings of IEEE Int. Symposium on EMC*, 1997, pp. 38–43.